18TH WORLD CONFERENCE ON EARTHQUAKE ENGINEERING
WCEE2024
MILAN

MILAN, ITALY
30TH JUNE - 5TH JULY 2024

www.wcee2024.it

MICROTREMOR MEASUREMENTS AND NUMERICAL MODELLING OF A TALL TIMBER-CONCRETE HYBRID BUILDING

Y. Miyazu[1] & C. Loss[2]

[1] Tokyo University of Science, Noda, Japan, miyazu@rs.tus.ac.jp

[2] The University of British Columbia, Vancouver, Canada, cristiano.loss@ubc.ca

Abstract: *Timber used as a structural material in high-rise buildings could add valuable bio-based alternatives for the development of sustainable cities. Particularly, timber-concrete hybrid (TCH) structures represent an efficient and practical solution to attain target structural performance, such as serviceability and seismic performance code requirements, by combining elements made of timber and concrete. The vibration properties—natural frequencies, damping ratios, and mode shapes—are fundamental parameters in the lateral design of buildings; however, these data are limited at this time for high-rise TCH buildings. In this research, microtremor measurements of an 18-story TCH building (UBC Brock Commons, Canada) were performed, and its vibration properties were identified via a stochastic subspace identification (SSI) procedure. A finite element (FE) model of the building was developed based on the structural design information to estimate its natural frequencies and mode shapes, and to perform modal time history analyses. The experimental results showed that the damping ratios remain between 1% and 3%, up to the eighth mode, and a 10% larger fundamental lateral period is estimated using the empirical formula provided in the 2020 National Building Code of Canada. The numerical study showed that a 2% constant damping ratio could provide a reliable estimation of the building's seismic response. In addition, the non-structural components significantly affected the fundamental frequency and the inter-story drift response in the longitudinal direction of the reference building. The findings provide practitioners with an insight into the vibration properties of high-rise TCH buildings and pave the way for developing reliable numerical models for the seismic design of TCH structures.*

1. Introduction

1.1. Tall mass timber and hybrid structures

Nowadays, glued laminated timber (GLT), cross-laminated timber (CLT), parallel strand lumber (PSL), and many other panel-like engineered wood products are used in mid-to high-rise timber construction. The material quality and mechanical properties of such products are well-checked through their manufacturing process. In addition, as engineered wood products, stiffness and strength, dimensional stability, and variation of mechanical properties are improved compared to their traditional solid wood counterparts.

With lightweight engineered wood products used as structural members, mass timber buildings have been widely accepted as a reasonable alternative to conventional concrete or steel buildings even in the countries located in regions prone to seismic hazards; however, constructing mid- to high-rise buildings using only timber as structural material may result in solutions structurally and technically challenging.

In mid-to high-rise timber buildings, hybrid lateral load-resisting systems (LLRS) have also been commonly used to ensure enhanced seismic performance and to increase the feasibility of the construction project. According to a survey by the Council on Tall Buildings and Urban Habitat (CTBUH), over 50% of tall timber buildings have concrete or steel coupled with timber structural members (Safarik et al. 2022). Specifically, timber-concrete hybrid (TCH) structural systems with concrete cores represent a reasonable solution for tall timber buildings, and it has already been introduced in a variety of tall timber projects, such as Brock Commons in Canada and Ascent in the United States. However, lateral performance and dynamic behaviour of TCH buildings are not well understood yet, mainly due to the lack of vibration data from actual building systems. To provide practitioners with confidence in designing and assessing the structural performance of such hybrid buildings, access to system-design parameters is compelling, such as dynamic properties obtained via vibration tests on actual built structures.

1.2. Seismic analysis and design of tall timber buildings

The National Building Code of Canada (NBC) (NRC 2020) directs designers to adopt dynamic analyses when assessing the lateral response of a building and to calculate solicitations in the members using the response spectrum method. When the building meets the design criteria specified in the building code, the equivalent static force procedure is also used by practitioners to derive the elastic forces in the members. Although the equivalent static force procedure is applicable to tall TCH buildings as long as these criteria are satisfied, it only applies to standard design cases built with conventional construction methods.

In encouraging innovative structural solutions for tall timber buildings, a performance-based seismic design (PBSD) framework is the most attractive and practical way for structural design. In the PBSD, time history response analysis is an indispensable method to obtain the deformation and acceleration responses of the building and estimate its safety and serviceability levels. The numerical model of the building used in the time history analysis should simulate the dynamic behaviour of the building as precisely as possible to ensure the reliability of the analytical results; however, there are some difficulties in the numerical modelling of the TCH buildings owing to their vibration properties.

1.3. Modelling of timber buildings

A systematic review of the modeling methods for tall mass timber buildings has been provided by Chen et al. (2022). With specific reference to buildings with CLT LLRS, *ad hoc* modeling techniques usually qualify for CLT panels (Saavedra Flores et al. 2016), CLT components using shear connectors (Feujofack and Loss 2023), and connection between CLT panels (Breneman et al. 2016), with static or pseudo-static plastic properties assigned mainly to their connections.

Regarding performing dynamic analyses, the scarcity of reliable vibration data acquired from on-site tests on actual buildings pushes for assumptions made based on engineering judgment. As an example, the knowledge of the damping ratio, including higher modes and the influence of non-structural components on the structural performance of tall timber buildings, is limited, except for case studies published in (Manthey et al. 2021, Tulebekova et al. 2022, Larsson et al. 2023).

To precisely estimate the seismic response of tall timber buildings, there is a need for knowledge of modal damping values, effects of higher modes, and stiffness of non-structural components on the LLRS behavior in order to provide the basis for a reliable design of the next generation of hybrid timber-based construction.

2. Method

2.1. Building overview

In this work, the UBC *Brock Commons Student Housing*, located in Vancouver, Canada, within the University of British Columbia campus (naturally:wood 2016), is used as a building archetype. With its 18-story TCH structural system, the building is known as one of the tallest mass timber buildings in the world. Figure 1a shows the exterior view from the northeast side of the building, whereas Figure 1b illustrates the 3D structural model of the superstructure. The podium and the two staircases are made of reinforced concrete (RC), while the columns and the floor panels of the superstructure are made of engineered wood, such as GLT, PSL, and CLT. The two RC cores were designed to download earthquakes and wind loads into the ground, whereas the CLT floors were detailed to act as diaphragms, transferring the lateral loads to the RC cores. The building gravity design was assumed with vertical loads to be transferred into the RC podium.

The building's footprint is 840 m^2 (15 m × 56 m), for a roof-to-ground height of 53 m. With regards to the timber floors, i.e., 2nd to 18th floors, the story height is 2.8 m, and the typical structural bay is 4 m × 2.85 m. Timber columns have a cross-section of 265 mm × 265 mm in the lower and 265 mm × 215 mm in the upper levels. The PSL columns, which have a higher Young's modulus than the GLT columns, are used at the central area in the lower levels to endure large axial forces. The 5-ply CLT floor panels are 169 mm thick. The mechanical properties of these materials are provided in Section 2.3. Specific design data, such as the foundation design, the floor design, and the configuration of the connections, can be found in Fast et al. (2016), Poirier et al. (2016), and Tannert and Moudgil (2017).

2.2. Microtremor measurements

Natural frequencies, damping ratios, and mode shapes of the reference building were assessed via ambient vibration testing (Miyazu and Loss 2023a). Eight servo velocity sensors, type VSE-15D produced by Tokyo Sokushin, and a data acquisition system, type SPC-52 produced by Tokyo Sokushin, were used to measure its lateral vibration properties. The velocity sensors were placed within the two RC cores for Cases 1 and 2, and on the 18th floor for Case 3, as illustrated in Figure 2. The testing program was conducted between March 27th and 29th, 2023. The vibration in the X- and Y-directions, which correspond to the longitudinal and the transverse directions of the building, were obtained in Cases 1 and 2. In contrast, only the Y-directional vibration was measured in Case 3, aiming to measure the torsional vibration of the building and the in-plane deformation of the top floor diaphragm. In each measurement, the elevator in the west-side RC core was turned off for 10 minutes in order to restrict the movement of residents and to avoid noise in the data. The sampling frequency was set at 200 Hz in all the tests.

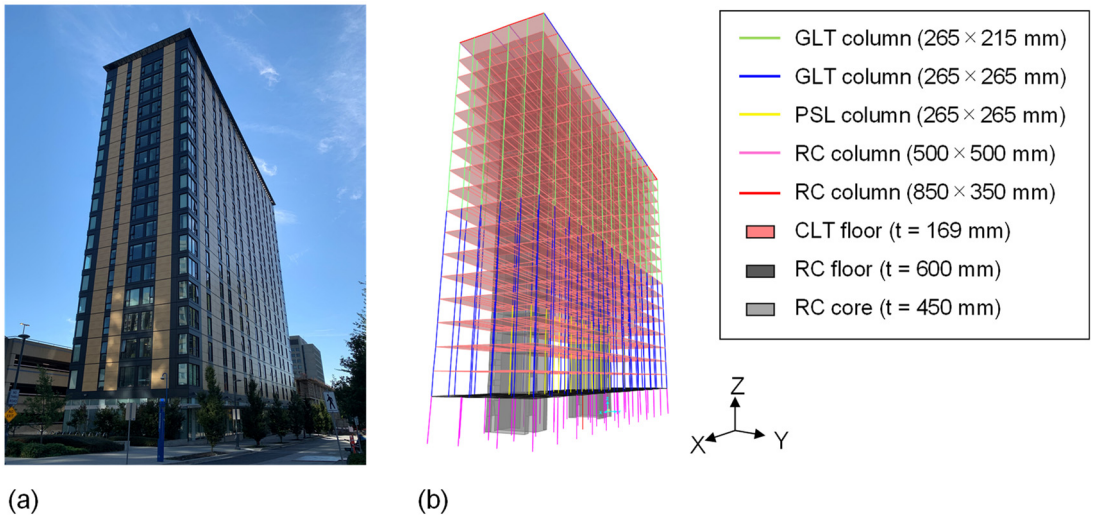

Figure 1. The 18-story tall timber-concrete hybrid building: (a) Exterior view, (b) 3D structural model.

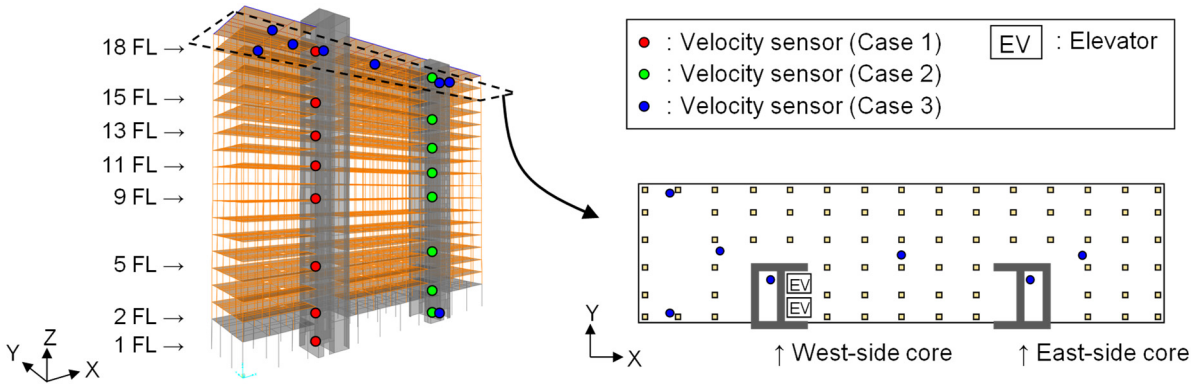

Figure 2. Location of velocity sensors.

Stochastic subspace identification (SSI) method proposed by Overschee and Moor (1996) was used to evaluate building's natural frequencies, damping ratios, and mode shapes. The model order *n* and the number of brock rows of the brock Hankel matrix *s* were varied from 100 to 200 and from 150 to 200, respectively. The identified values satisfying Equations 1 to 3 were considered stable modes.

$$\frac{\left|{}_{q}f_{r}-{}_{q}f_{r+4}\right|}{{}_{q}f_{r}}\le 0.05 \quad \cap \quad \frac{\left|{}_{q}f_{r}-{}_{q+10}f_{r}\right|}{{}_{q}f_{r}}\le 0.05 \tag{1}$$

$$\frac{\left|{}_{q}h_{r}-{}_{q}h_{r+4}\right|}{{}_{q}h_{r}}\le 0.1 \quad \cap \quad \frac{\left|{}_{q}h_{r}-{}_{q+10}h_{r}\right|}{{}_{q}h_{r}}\le 0.1 \tag{2}$$

$$\frac{\left|{}_{q}\boldsymbol{\varphi}_{r}^{*}\,{}_{q}\boldsymbol{\varphi}_{r+4}\right|^{2}}{\left({}_{q}\boldsymbol{\varphi}_{r}^{*}\,{}_{q}\boldsymbol{\varphi}_{r}\right)\left({}_{q}\boldsymbol{\varphi}_{r+4}^{*}\,{}_{q}\boldsymbol{\varphi}_{r+4}\right)}\ge 0.95 \quad \cap \quad \frac{\left|{}_{q}\boldsymbol{\varphi}_{r}^{*}\,{}_{q+10}\boldsymbol{\varphi}_{r}\right|^{2}}{\left({}_{q}\boldsymbol{\varphi}_{r}^{*}\,{}_{q}\boldsymbol{\varphi}_{r}\right)\left({}_{q+10}\boldsymbol{\varphi}_{r}^{*}\,{}_{q+10}\boldsymbol{\varphi}_{r}\right)}\ge 0.95 \tag{3}$$

where ${}_{q}f_{r}$, ${}_{q}h_{r}$, and ${}_{q}\boldsymbol{\varphi}_{r}$ are the natural frequency, damping ratio, and mode vector with $n=r$ and $s=q$, respectively. The last criterion evaluates a modal assurance criterion (MAC), where superscript (*) denotes complex conjugate transpose. The detailed information of this test, such as the measurement program, the data processing, and the identified results, are presented in Miyazu and Loss (2023b).

2.3. Numerical modelling

In SAP2000 (CSI 2023), the three-dimensional FE model of the building was developed by crossing data from the structural, shop, and construction drawings. The FE model consists of four parts, including timber members, reinforced concrete elements, claddings, and partition walls, as shown in Figures 3a to 3d. In the timber and concrete parts, the columns were modeled with beam-type elements, while the walls and floors were modeled with four-node thick-shell elements based on Reissner-Mindlin's plate theory. The claddings and the partition walls were represented by elastic link-type elements installed diagonally between two nodes.

The stress grades of GLT and PSL are 16c-E and 2.2E, respectively. The CLT panel has two outer and three inner layers, and their stress grades are E2 and V2, respectively. A Layered shell element was applied to the CLT panel to account for the different mechanical properties of each layer, as shown in Figure 4a. 6 m, 8 m, 10 m, and 12 m long elements were used for the CLT floor panels, with geometry accounting for the actual openings, as illustrated in Figure 4b. The mechanical properties of the elements used in the model are listed in Table 1. The stiffness of the link elements simulating the cladding and partition walls was assigned in order to minimize the difference between the numerical and experimental values of the first three natural frequencies. Connections between the two CLT panels, as well as between the CLT panels and the RC cores, were assumed to be rigid in tension, compression, and shear, while the out-of-plane moment at their edges was released. Regarding dead loads, 2.25 kPa for rooms, 1.25 kPa for corridors, and 0.9 kPa for roofs were assigned in compliance with the design documentation. As for live loads, 0.36 kPa for rooms, 0 kPa for corridors and the roof were estimated based on the architectural layout and the actual service condition.

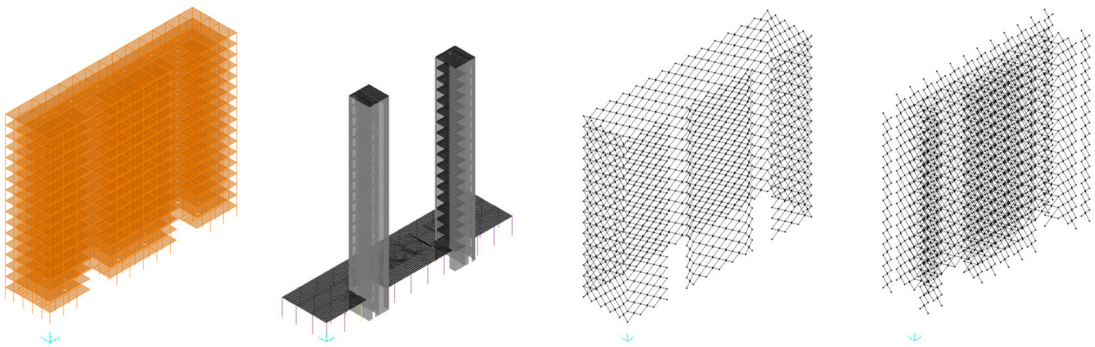

Figure 3. Finite-element model: (a) Timber members, (b) Reinforced Concrete elements, (c) Claddings, (d) Partition walls.

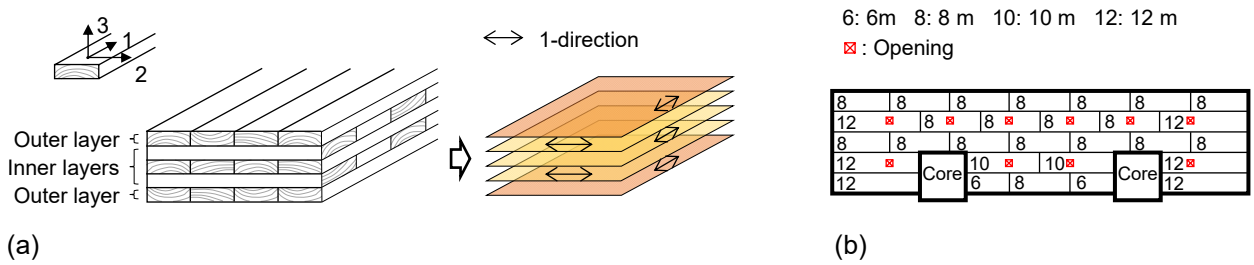

Figure 4. Modelling of CLT panels: (a) Layered shell model, (b) Arrangement of CLT floor panels.

Table 1. Mechanical properties of the elements used in the FE model.

Property (Unit)	RC	GLT	PSL	CLT		Link element	
				Outer layer	Inner layer	Cladding	Partition wall
E (MPa)	26,620	12,400	15,100	—	—	—	—
G (MPa)	11,090	—	—	—	—	—	—
E_1 *(MPa)*	—	—	—	10,300	9,500	—	—
E_2, E_3 *(MPa)*	—	—	—	343	317	—	—
G_{12}, G_{13} *(MPa)*	—	—	—	644	594	—	—
G_{23} *(MPa)*	—	—	—	64	59	—	—
k_c, k_p *(kN/mm)*	—	—	—	—	—	k_c = 7	k_p = 12

2.4. Ground motion selection

Seismic hazard analysis and ground motion selection were carried out in compliance with the National Building Code of Canada 2020 (NRC 2020), a procedure highlighted in Tesfamariam et al. (2023). OpenQuake (GEM 2022) was used to generate the uniform hazard spectrum and the disaggregation results at the building site based on the 6th generation seismic hazard model developed by Natural Resources Canada (Kolaj et al. 2020). To select the occasional earthquakes level (SEAOC 1999), the probability of exceedance in 50 years was set to 50%, i.e., the return period is 72 years. Figures 5a and 5b show the generated uniform hazard spectrum and the disaggregation for intensity measure $S_a(1.0)$, respectively.

Ten ground motions were selected based on the conditional mean spectrum (Baker 2011) using the source code provided by Baker and Lee (2018). The conditioning period was determined at 1.0 second based on the fundamental period of the building. The period range [T_{min}, T_{max}] was defined as [0.2, 2]. PEER NGA-West2 Database was used as the earthquake database for the ground motion selection. Table 2 lists the selected 10 ground motions and their response spectrum are plotted in Figure 5c.

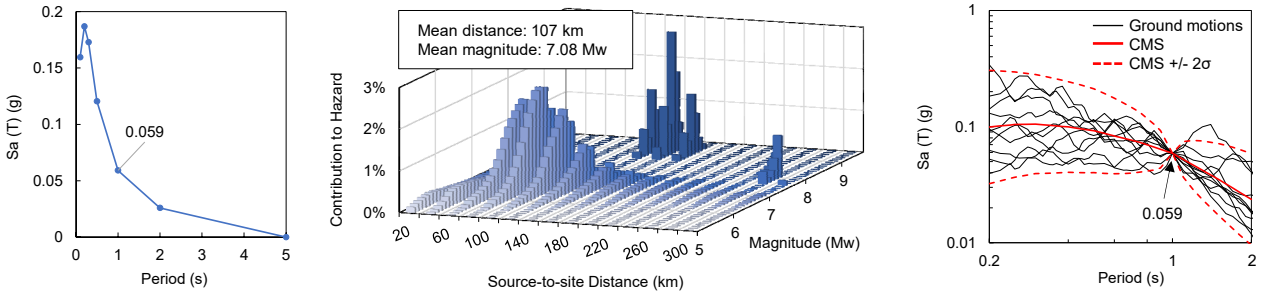

Figure 5. Probabilistic seismic hazard analysis and ground motion selection: (a) Uniform hazard spectrum at the building site, (b) Disaggregation for intensity measure $S_a(1.0)$, (c) Response spectrum of selected ground motions (h = 0.05).

Table 2. Selected ground motions.

No.	Earthquake Record	Year	Station Name	Magnitude	Mechanism
1	Imperial Valley-06	1979	Chihuahua	6.53	Strike slip
2	Nahanni_ Canada	1985	Site 1	6.76	Reverse
3	Chalfant Valley-02	1986	Long Valley Dam (Downst)	6.19	Strike slip
4	Northridge-01	1994	LA 00	6.69	Reverse
5	Kobe_ Japan	1995	Kakogawa	6.9	Strike slip
6	Chi-Chi_ Taiwan	1999	CHY092	7.62	Reverse oblique
7	Chi-Chi_ Taiwan	1999	HWA005	7.62	Reverse oblique
8	Chi-Chi_ Taiwan-06	1999	TCU065	6.3	Reverse
9	Iwate_ Japan	2008	Matsuyama City	6.9	Reverse
10	L'Aquila_ Italy	2009	Fiamignano	6.3	Normal

2.5. Modal time history analysis

To evaluate the effect of the damping ratio and the non-structural component elastic properties changes on the building's seismic responses, modal time history analyses were performed in SAP2000. Closed-form integration was set to solve the system's equation of motion. The number of modes considered in the analysis was set to 23, including second X- and Y-translational modes and second torsional mode around the Z-axis, as well as the in-plane bending modes of the CLT diaphragms. Table 3 summarizes the parameters varied in the modal time history analysis. With reference to Table 3, model STD has damping ratio values evaluated by the vibration tests and effect of non-structural components included, and stands for the best approximation to the actual vibration response of the building. Models H1, H2, and H3 have damping ratios with constant values in all the modes, representing practical damping values used in the lateral structural design. Model NN is added to assess the effect of the stiffness of the non-structural components, and has a 2% damping ratio set to all the modes. In Section 3.2, results from model NN analysis are compared with those of model H2. A set of 20 ground motion records (bi-directional records for one ground motion) were inputted separately in the X- and Y-directions.

Table 3. Analysis models.

Name	Damping ratios	Non-structural components
STD	Test results*	Included
H1	1% in all the modes	Included
H2	2% in all the modes	Included
H3	3% in all the modes	Included
NN	2% in all the modes	Not included

*The values shown in Table 4

3. Results and discussion

3.1. Dynamic properties

The natural frequencies and the damping ratios identified through the microtremor measurements and post-processing via SSI data analysis are summarized in Table 4. The natural frequencies and the participation mass ratios computed with the eigenvalue analysis on model STD are also included for reference. For model NN, natural frequencies of the 1st, 2nd, 3rd, 4th, 14th, 16th, 22nd, and 37th modes, the mode shapes of which correspond to those of model STD, are shown to compare with model STD. Figure 6 illustrates the mode shapes of the selected eight modes in which the building's lateral vibration dominates. Note that the mode shapes of model STD agree well with those evaluated by Miyazu and Loss (2023b).

The extracted natural frequencies of model STD show good agreement with those assessed by testing, and the damping ratios corresponding to the natural frequencies show being distributed between 1% and 3%. These damping ratios were used in the modal time history analysis of model STD. From the mode shapes of Figure 6 and the participating mass ratios in Table 4, the 1st and the 4th modes are the X-translational modes, while the 2nd and the 8th modes are the Y-translational modes. The 3rd and the 10th modes show the torsional modes around the Z-axis. In the 13th and the 23rd modes, the in-plane bending of the CLT floor diaphragm is

shown in their mode shapes. The difference between the natural frequencies of the 1st translational and torsional modes is only 20%, featuring a higher likelihood of coupling effects under dynamic excitations of the building. When comparing NN with STD models, the inherent stiffness of the non-structural components mainly affects the 1st translational mode in the X-direction and increases its frequency by 23%.

NBC2020 (NRC 2020) provides a formula to estimate the fundamental period of a building with shear walls as follows:

$$T_{NBC} = 0.05H^{3/4} \quad (4)$$

where H is the building's height (expressed in m).

For the 53 m tall building, the estimated fundamental frequency is 1.02 Hz, 10% larger than the identified natural frequency of the 1st mode. Although the TCH system is not covered explicitly in this formula, the estimated value gives a good approximation of the test results. However, more building samples and analysis are required to validate the applicability of this formula to tall TCH buildings.

Table 4. Natural frequencies, damping ratios, and participating mass ratios of the reference building.

		Mode							
		1	2	3	4	8	10	13	23
Natural Frequency (Hz)	FE model (STD)	0.93	0.95	1.17	3.85	4.61	4.81	5.27	6.53
	Test result	0.93	0.94	1.16	3.80	4.49	4.82	5.77	6.10
	FE model (NN)	[1]	[2]	[3]	[4]	[14]	[16]	[22]	[37]
		0.72	0.90	1.08	3.55	4.48	4.61	5.19	6.27
Ratio of natural frequency = FE model (STD) / Test result		1.0	1.01	1.01	1.01	1.03	1.0	0.91	1.07
Ratio of natural frequency = FE model (NN) / FE model (STD)		0.77	0.95	0.92	0.92	0.97	0.96	0.98	0.96
Damping ratio evaluated by the test (%)		1.2	1.1	1.3	2.5	2.3	2.4	2.8	1.1
Participating mass ratio of mode STD (%)	U_x	55	1	5	15	0	3	1	0
	U_y	0	58	0	0	20	1	0	0
	R_z	5	0	55	4	1	12	0	0

* Numbers in brackets indicate the mode order of model NN.

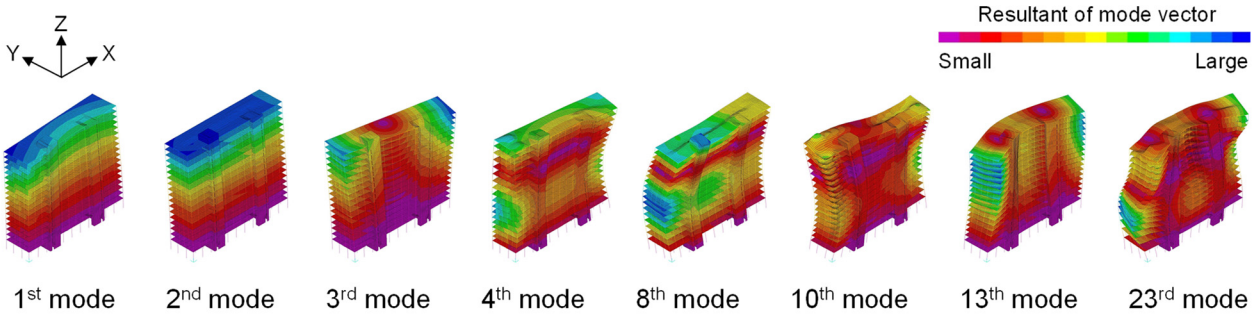

Figure 6. Mode shapes of model STD.

3.2. Seismic response

Model STD

Figure 7 shows the maximum inter-story drift (ISD) ratio and the maximum absolute acceleration (AA) response in each direction at the selected nodes obtained from the modal time history analysis of the STD model. The selected nodes are indicated by black circles at one corner of the building. With reference to the plots of Figure 7, the averages of maximum ISD and AA from the 20 ground motion records are provided in solid red lines in the two main directions, whereas the dashed red lines show the results by adding the standard deviation to the average values. Individual results from the suite of ground motion are provided in grey continuous lines.

Figure 8 reports the Fourier amplitudes of the displacement and the absolute acceleration at the selected node on the rooftop (19th floor).

In the X- and Y-directions, regardless of the ground motion and story level, the maximum ISD is recorded below 0.2%; thus, the lateral deformation of the building remained elastic and without damage in the non-structural components. The ISD is shown to be larger in the upper stories as per systems in which the bending deformation dominates their lateral deflection. The peak dominant frequency of around 1 Hz in both directions extracted from the Fourier amplitude of the displacement at the 19th floor confirms that the displacement response is governed by the first mode. With regards to the AA, the maximum values at the 9th and the 19th floors are shown larger than those at the 15th floor and scattered. With reference to the Fourier amplitude expressed in acceleration, results showed second peaks around 3.8 Hz in the X-direction and 4.5 Hz in the Y-direction, respectively. These frequencies corresponded to the second modes of the building in each direction. Such results suggest that the first and second modes should be considered in order to obtain an accurate estimate of the total acceleration response.

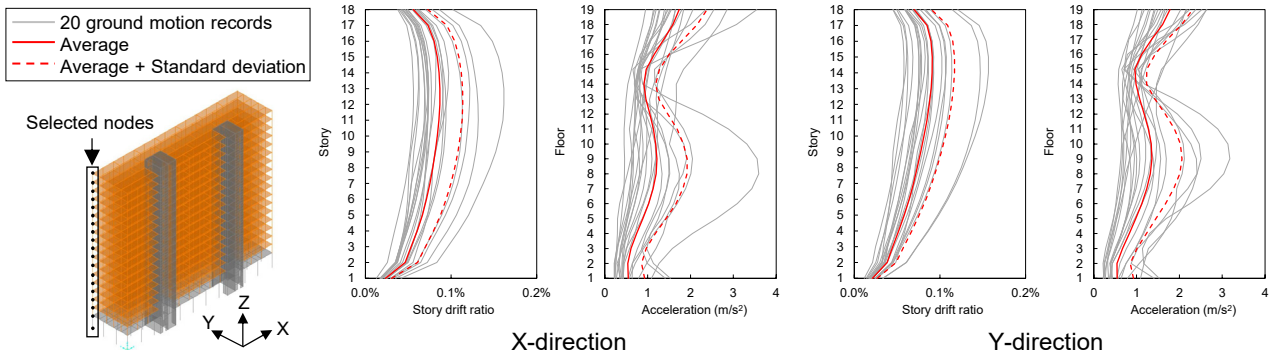

Figure 7. Maximum inter-story drift ratio and acceleration of model STD in the X- and the Y-directions.

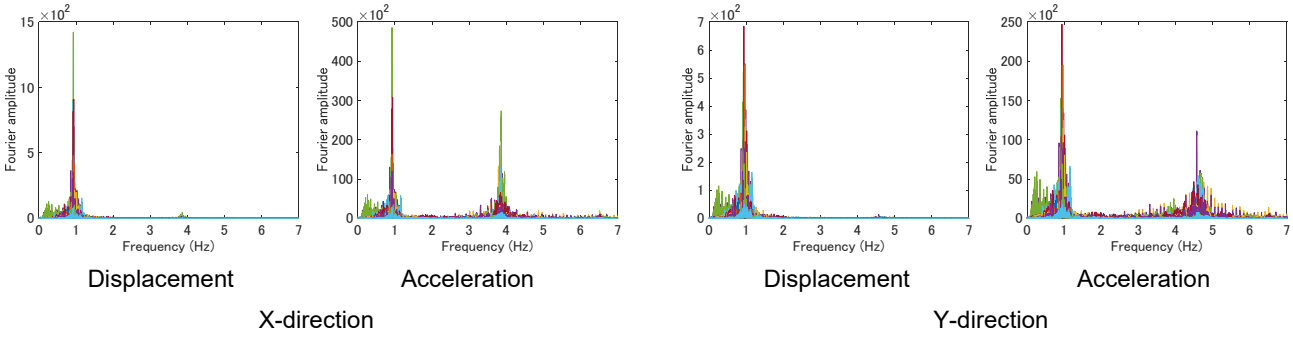

Figure 8. Fourier amplitudes of the displacement and the acceleration at the 19th floor in the X- and the Y-directions.

It is worth noting that the maximum ISD remained below 0.4%, confirming that the structural damage is generally expected to be negligible and the performance objective is above Enhanced Objective 1 (EO1) defined in the SEAOC (1999).

Effect of damping ratio

Figure 9 illustrates the average of the maximum ISD and AA of the four models: STD, H1, H2, and H3. Such plots provide visual patterns of the ISD and AA to the modal damping ratio. Figure 10 shows the difference between model STD and other models, defined by parameter *D*, obtained as follows:

$$D = \frac{(R - R')}{R'} \tag{5}$$

where *R'* and *R* are the responses of model STD and other models, respectively. In model H2, the maximum *D* is about 10% in both the maximum IDA and AA, showing the best approximation to model STD. Structural

Commentaries of NBC2015 (NRC 2017) recommends using 2% damping for buildings with concrete frames when evaluating its wind response by dynamic analysis. Although the reference building is not a concrete frame structure, the result indicates that the 2% damping recommended in NBC2015 (NRC 2017) can be suitable for seismic response analysis on TCH buildings subjected to occasional earthquakes.

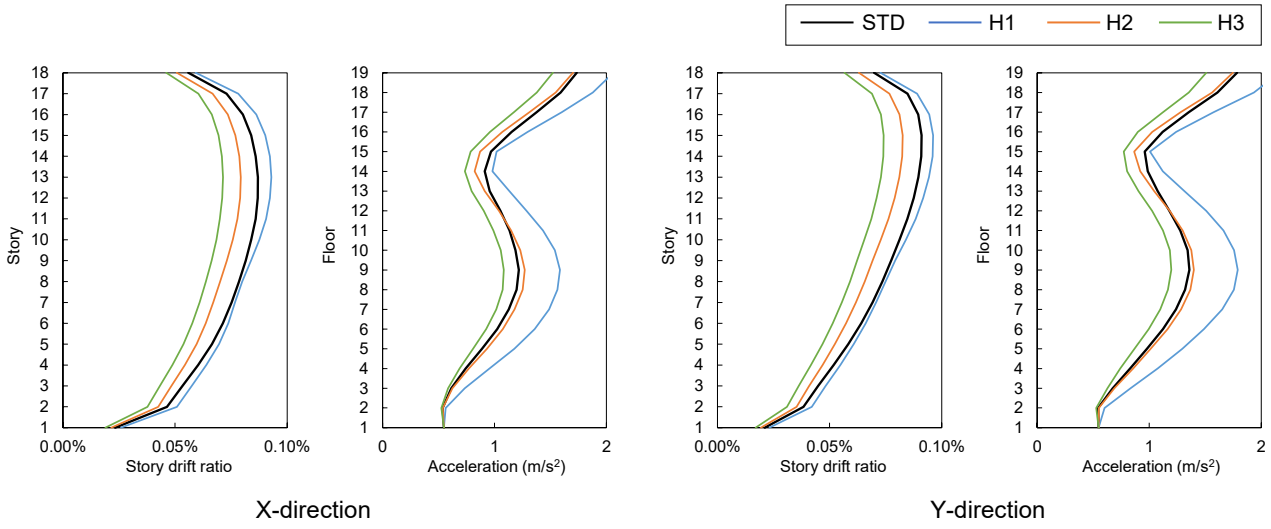

Figure 9. Average of maximum response of four models with different damping ratios.

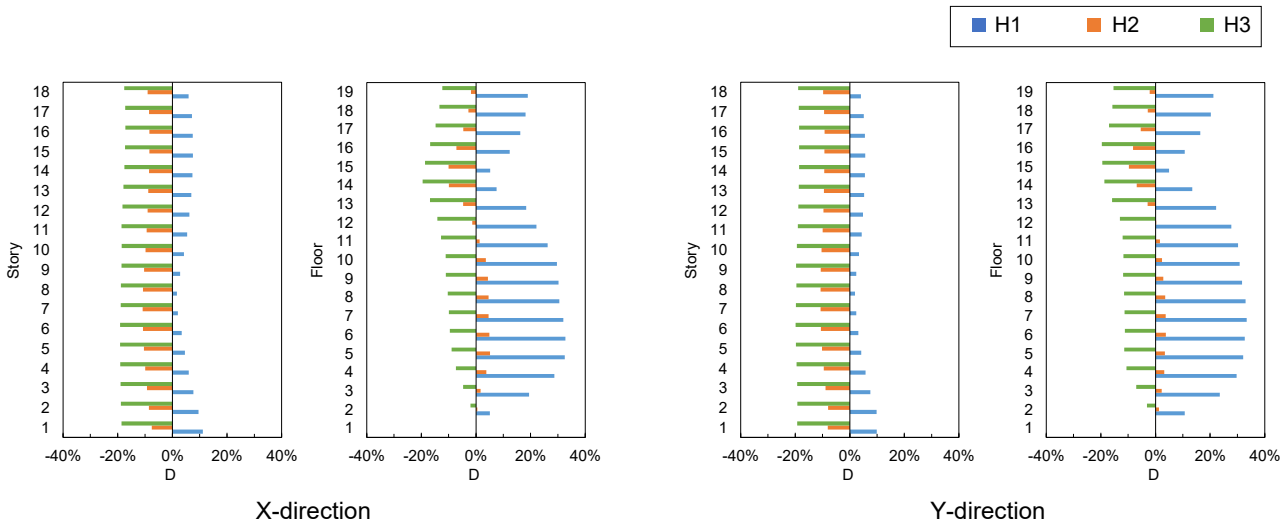

Figure 10. Difference of responses between model STD and other models.

Effect of non-structural components

In Figure 11, the influence of the non-structural components, i.e., the claddings and the partition walls, on the seismic responses of the building is assessed by comparing results from H2 and NN models. The difference between models H2 and NN calculated by Equation 5, where *R'* and *R* are the responses of H2 and NN, respectively, is also included. It is shown that the non-structural components have a more significant impact on the X-directional response than the Y-directional one, and the ISD is more sensitive to the non-structural components than the AA. The difference between the two models is the largest in the X-directional ISD response, and the value of *D* is about 100% at the 18th story.

As indicated in Table 4, the natural frequency in the 1st mode of model NN, which corresponds to the translational mode in the X-direction, became 77% of that of H2 when removing the link elements simulating the non-structural components, increasing the story drift ratio of model NN. As shown in Figure 5c, the

acceleration response spectrum is almost flat in the range from 3 Hz (0.33 s) to 5 Hz (0.2 s), where the 2nd mode exists; therefore, the difference of the AA was not shown to be significant.

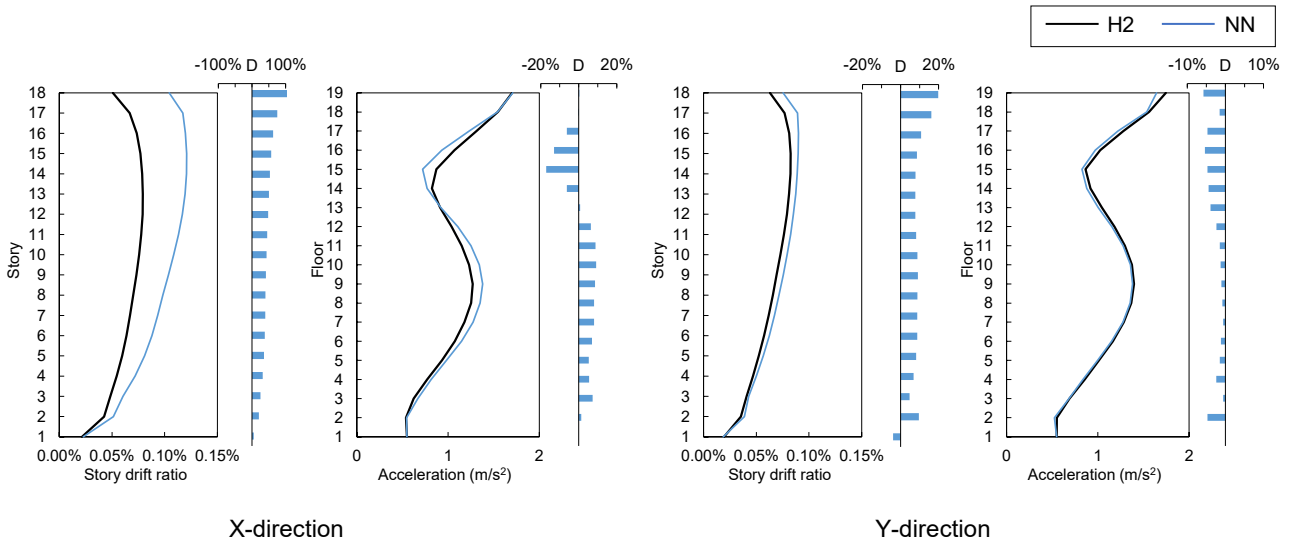

Figure 11. Effect of the non-structural components on the ISD and AA.

According to NBC2020 (NRC 2020), the stiffness of non-structural components should be considered in calculating the natural period of the building if the added stiffness decreases the fundamental lateral period by more than 15%. In the reference building, the stiffness of the non-structural components reduces the fundamental period by 23%; hence, the non-structural components should be considered in the structural model to comply with NBC2020 (NRC 2020). Since the stiffness of non-structural components highly depends on their arrangement, it is desired to assess the stiffness in advance of the structural design through experimental or analytical studies.

4. Conclusions

In this research, an FE model of an 18-story TCH building was developed and tailored to the lateral vibration data obtained by microtremor measurements of the actual building. Its seismic responses to a suite of selected ground motions were evaluated through modal time history analyses. The following conclusions can be drawn:

- The damping ratios identified through the on-site vibration tests were assessed between 1% and 3%, even for the higher modes. NBC2015 recommends assigning a 2% damping for concrete frame structures when estimating lateral low-amplitude vibrations, which is compatible with these test results. The fundamental frequency was found to be equal to 0.93 Hz; thus, 10% smaller than the estimated value via the empirical formula for concrete frame structures provided in NBC2020
- The difference between the natural frequencies of the 1st translational and torsional modes was 20%, indicating that the coupling of the two modes could easily occur under dynamic loading
- The maximum inter-story drift ratio was recorded below 0.2% under excitations caused by occasional earthquakes. The inter-story drift was governed mainly by the 1st mode, while the acceleration response was affected by both the 1st and 2nd modes
- The FE model with 2% damping assigned in all the modes showed good coherence with the model built using damping ratios identified from the test series
- The decrease of the fundamental period by adding the non-structural components was 23%, exceeding the reference value stipulated in NBC2020. The stiffness of the non-structural components significantly affected the inter-story drift in the longitudinal direction of the building.

5. Acknowledgements

This research was funded by the Government of British Columbia through the FII Wood First Program, and by the Natural Sciences and Engineering Research Council (NSERC) of Canada through the Discover Program

grant number RGPIN-2019-04530, and Discovery Launch Supplement, grant number DGECR-2019-00265. The authors are also grateful to Asghar AmaniDashlejeh, David Owolabi, Blériot Feujofack, Yue Diao, Demin Feng, Tomomasa Komatsubara, Takehiro Wakita, Hideyuki Kinugasa, Masayuki Nagano, Yoshifumi Ohmiya, and Ai Tomita for their contribution throughout the testing program. The authors would also like to thank Diana Lopez, David Kiloh, Angelique Pilon, Andrew Powter, Andrew Parr, and John Metras for their support in scheduling and coordinating the on-site testing program.

6. References

Baker J.W. (2011). Conditional mean spectrum: tool for ground-motion selection, *Journal of Structural Engineering*, 137(3): 322–331.

Baker J.W., Lee C. (2018). An Improved Algorithm for Selecting Ground Motions to Match a Conditional Spectrum, *Journal of Earthquake Engineering*, 22(4): 708-723.

Breneman S., McDonnell E., Zimmerman R. (2016). An approach to CLT diaphragm modelling for seismic design with application to a US high-rise project, *Proceedings of the Word Conference on Timber Engineering 2016 (WCTE 2016)*, 3812-3120.

Chen Z., Tung D., Karacabeyli E. (2022). *Modelling Guide for Timber Structures*, Vancouver: FPInnovations.

Computers and Structures, Inc. (CSI) (2023). *SAP2000 version 24.2.0.* California.

Fast P., Gafner B., Jackson R., Li J. (2016). Case study: An 18 story tall mass timber hybrid student residence at the University of British Columbia, *Proceedings of the Word Conference on Timber Engineering 2016 (WCTE 2016)*, Vienna, Austria.

Feujofack B., Loss C. (2023). Finite-Element Modelling of a Novel High-Performance Shear Connector for Mass Timber Structural Assemblies, *Proceedings of the Canadian Society of Civil Engineering Annual Conference 2022 (CSCE 2022)*, Whistler, Canada.

GEM (2022). The OpenQuake-engine User Manual. *Global Earthquake Model (GEM) OpenQuake Manual for Engine version 3.17.2*, doi: 10.13117/GEM.OPENQUAKE.MAN.ENGINE. 3.17.2.

Kolaj M., Halchuk S., Adams J., Allen T.I. (2020). Sixth Generation seismic hazard model of Canada: Input files to produce values proposed for the 2020 National Building Code of Canada, *Geological Survey of Canada, Open File 8630*, 1 .zip file.

Larsson C., Abdeljaber O., Dorn M. (2023). Dynamic evaluation of a nine-storey timber-concrete hybrid building during construction, *Engineering Structure*, 289:116344.

Manthey M., Flamand O., Jalil A., Pavic A., Ao W. K. (2021). Effect of Non-Structural Components on Natural Frequency and Damping of Tall Timber Building under Wind Loading, *Proceedings of the Word Conference on Timber Engineering 2021 (WCTE 2021)*, Santiago, Chile.

Miyazu Y., Loss C. (2023a). Lateral vibration data of an 18-story timber-concrete hybrid building obtained by on-site vibration tests, *Data in Brief*, 50.

Miyazu Y., Loss C. (2023b). Evaluation of vibration properties of an 18-story mass timber-concrete hybrid building by on-site vibration tests, *Journal of Civil Structural Health Monitoring*, In Press.

naturally:wood (2016) Tallwood House Storyboards, https://www.naturallywood.com/wp-content/uploads/brock-commons-storyboards_factsheet_naturallywood.pdf, Accessed 25 May 2023.

NRC (2017). *Structural Commentaries (User's Guide – NBC 2015: Part 4 of Division B)*, National Research Council of Canada, Ottawa.

NRC (2020). *National Building Code of Canada (NBC) 2020.* National Research Council of Canada, Ottawa.

Overschee P.V., Moor B.D. (1996). *Subspace Identification for Linear Systems: Theory, Implementation and Applications*, Amsterdam: Kluwer Academic Publishers.

Poirier E., Moudgil M, Fallahi A., Staub-French S., Tannert T. (2016). Design and Construction of a 53-meter-tall Timber Building at the University of British Columbia, *Proceedings of the Word Conference on Timber Engineering 2016 (WCTE 2016)*, Vienna, Austria.

Saavedra Flores E.I., Saavedra K., Hinojosa J., Chandra Y., Das R. (2016). Multi-scale modelling of rolling shear failure in cross-laminated timber structures by homogenisation and cohesive zone models, *International Journal of Solids and Structures*, 81, 219-232.

Safarik D., Elbrecht J. (2022). Miranda W. State of tall timber 2022, https://www.ctbuh.org/resources/papers/4530-Journal2022_Issue1_StateofTallTimber+TBIN.pdf, Accessed 22 August 2023.

Structural Engineers Association of California (SEAOC). (1999). *Recommended Lateral Force Requirements and Commentary*, Seventh Edition, California: SEAOC.

Tannert T., Moudgil M. (2017). Structural Design, Approval, and Monitoring of a UBC Tall Wood Building, *Structure Congress 2017*, 541-547.

Tesfamariam S., Badal P.S., Goda K. (2023). Seismic Hazard and Ground Motion Selection for Response History Analysis based on the National Building Code of Canada 2020, *UBC Faculty Research and Publications*.

Tulebekova S., Malo K. A., Rønnquist A., Nåvik P. (2022). Modeling stiffness of connections and non-structural elements for dynamic response of taller glulam timber frame buildings, *Engineering Structure*, 261:114209.